AIP | Journal of Applied Physics

An influence of the local strain on cathodoluminescence of GaN/AlxGa1−xN nanowire structures

Anna Reszka, Aleksandra Wierzbicka, Kamil Sobczak, Uwe Jahn, Ute Zeimer, Andrian V. Kuchuk, Agnieszka Pieniążek, Marta Sobanska, Kamil Klosek, Zbigniew R. Zytkiewicz, and Bogdan J. Kowalski

Citation: Journal of Applied Physics **120**, 194304 (2016); doi: 10.1063/1.4968004
View online: http://dx.doi.org/10.1063/1.4968004
View Table of Contents: http://scitation.aip.org/content/aip/journal/jap/120/19?ver=pdfcov
Published by the AIP Publishing

An influence of the local strain on cathodoluminescence of GaN/$Al_xGa_{1-x}N$ nanowire structures

Anna Reszka,[1,a)] Aleksandra Wierzbicka,[1] Kamil Sobczak,[1] Uwe Jahn,[2] Ute Zeimer,[3] Andrian V. Kuchuk,[4,5] Agnieszka Pieniążek,[1] Marta Sobanska,[1] Kamil Klosek,[1] Zbigniew R. Zytkiewicz,[1] and Bogdan J. Kowalski[1]

[1]*Institute of Physics, Polish Academy of Sciences, Aleja Lotnikow 32/46, PL-02668 Warsaw, Poland*
[2]*Paul-Drude-Institut für Festkörperelektronik, Hausvogteiplatz 5–7, D-10117 Berlin, Germany*
[3]*Ferdinand-Braun-Institut, Leibniz-Institut für Höchstfrequenztechnik, Gustav-Kirchhoff-Str. 4, D-12489 Berlin, Germany*
[4]*Institute for Nanoscience and Engineering, University of Arkansas, West Dickson 731, Fayetteville, Arkansas 72701, USA*
[5]*V. Lashkaryov Institute of Semiconductor Physics, National Academy of Sciences of Ukraine, Pr. Nauky 41, 03680 Kyiv, Ukraine*

(Received 10 August 2016; accepted 6 November 2016; published online 21 November 2016)

Near-band-edge excitonic emission shift is investigated as a measure of the local strain in GaN nanowires with single $Al_xGa_{1-x}N$ sections of various Al contents (x = 0.0, 0.22, 0.49, 1.0). Complementary data obtained by spatially and spectrally resolved cathodoluminescence spectroscopy and imaging of individual nanowires at low temperature, high resolution X-ray diffraction, and transmission electron microscopy are used to determine the correspondence between the cathodoluminescence emission energy and the strain in the GaN core of the nanowire surrounded by the $Al_xGa_{1-x}N$ shell formed during the growth of $Al_xGa_{1-x}N$ sections by catalyst-free plasma-assisted molecular beam epitaxy. In majority of nanowires, the blue-shift of GaN cathodoluminescence follows the evolution expected for the GaN core under uniaxial compressive strain along the axis of the structure. *Published by AIP Publishing.* [http://dx.doi.org/10.1063/1.4968004]

I. INTRODUCTION

It is well established that low-dimensional structures containing gallium nitride and its alloy with aluminum nitride are promising building blocks for novel optoelectronic nano-devices, among others, efficient high brightness light emitters.[1,2] For this purpose, the multilayer structures with a high crystalline quality are required, if possible, grown on easily accessible, low-cost substrates. Epitaxy of nitrides on silicon is particularly attractive due to the potential integration of GaN devices with contemporary advanced Si microelectronics. However, in such a system the considerable differences in lattice constants and thermal expansion coefficients lead to stress relaxation by creation of extended defects, degrading the basic electrical and optical parameters of the device. Replacing of the planar structures with nanowire (NW) ensembles is considered as a possible solution of that problem. The small contact area of NW with the substrate and the high surface-to-volume-ratio (free surface at the sidewalls) makes the elastic accommodation of lattice mismatch strain much easier. This leads to a significant reduction of the density or even an elimination of extended defects, which may notably improve the electrical and optical properties of nitride devices based on NWs, especially grown on silicon substrates.[3,4] The non-planar geometry of NWs allows also the fabrication of axial or radial heterostructures with barriers and wells of highly lattice mismatched material combinations.[2] However, growing complex axial structures with the use of molecular beam epitaxy (MBE) often leads also to an overgrowth of the side walls and creation of a radial structure of the core-shell type. In particular, for nitride nanowires with axial GaN/AlN junctions, due to the low surface mobility of Al adatoms, such radial overgrowth cannot be avoided.[5] Formation of shells in GaN/$Al_xGa_{1-x}N$ and GaN/AlN heterostructures was reported also by Himwas *et al.*[6] and Zagonel *et al.*[7] The presence of such shells results in the appearance of strain in the NWs. As all those features strongly influence the luminescence spectrum of the structure, proper assessment of their presence and strength is a precondition of a reproducible fabrication of devices based on NWs, such as nano-LEDs. The strains and their relaxation in the core-shell heterostructures were analyzed by theoretical methods[8] and studied, in particular, for some nitride systems, by experimental techniques probing structural and optical features of nanowires.[5,9,10] In Ref. 5, the strains in the GaN/$Ga_{1-x}Al_xN$ nanocavities were investigated by high resolution transmission electron microscopy (HRTEM), photo- and cathodoluminescence (CL). The nanocolumns with GaN/AlN core–shell heterostructures were studied by HRTEM, μ-Raman,[9] macro-, and μ-photoluminescence (PL).[10] The strains induced by the lattice constant misfit between GaN and AlN were estimated and correlated with shifts of Raman and PL spectral features.

In addition to the aforementioned experimental methods, cathodoluminescence (CL) is a useful technique, dedicated for studying the details of the systems with submicron dimensions.[11] It was successfully used to visualize a luminescence from the stacks of GaN/AlN quantum discs in nanowires.[7] It was also used in the studies of composition fluctuations in the

[a)]Author to whom correspondence should be addressed. Electronic mail: reszka@ifpan.edu.pl

$Al_xGa_{1-x}N$ nanodisks[6] or complex nanowires,[12,13] accompanied with the investigations of the latter by Raman, macro-, and μ-PL spectroscopies carried out in the whole range of Al contents.[14]

In the study reported in this paper, we extend the investigations of GaN nanowires with $Al_xGa_{1-x}N$ sections by CL, HRTEM, and high resolution X-ray diffraction (HRXRD) into the whole range of $Al_xGa_{1-x}N$ composition (for $x = 0$, 0.22, 0.49, 1.0). During the growth of $Al_xGa_{1-x}N$ segments, a shell of $Al_xGa_{1-x}N$ around the GaN-base of NW is formed. The lattice constant misfit between GaN and $Al_xGa_{1-x}N$ leads to strain in the structure and, as a consequence, to energy shifts of luminescence spectral features. Therefore, we focused the analysis of the acquired data on strain–luminescence correlation considered at a function of $Al_xGa_{1-x}N$ composition. For a GaN nanowire overgrown with the shell made of the solid solution, there are two related factors governing the stress imposed on the core: the solid solution composition and the shell thickness. We demonstrate that these factors acting simultaneously lead to a regular change of a strain in the core and the energy of luminescence of it. This dependence can be determined and accounted for in design of complex structures with $Al_xGa_{1-x}N$ elements. Segments grown on $Al_xGa_{1-x}N$ with various compositions play a crucial role in the NW-based optoelectronic devices as the components of heterostructures. We focus our interest on NWs with single $Al_xGa_{1-x}N$ sections having the length of the order of 100 nm, comparable with the thicknesses of the cladding or waveguiding elements of devices.

The vertically aligned GaN nanowires are grown catalyst-free on silicon substrates by plasma-assisted molecular beam epitaxy (PAMBE).[15,16] The structural and optical properties of the GaN/$Al_xGa_{1-x}N$ nanowire structures are studied by scanning electron microscopy (SEM), HRTEM, CL spectroscopy, and HRXRD technique. Spatially and spectrally resolved CL spectroscopy and imaging in the photon energy range of the near-band-gap excitonic emission are used to record the local energy shifts of the spectral features along NWs. The HRXRD experiments and determination of the accurate values of lattice parameters allow us to estimate the averaged strain state in GaN as well as in $Al_xGa_{1-x}N$ and to correlate it with CL emission of corresponding parts of the NW. All these results enable a detailed analysis of the strain distribution in the NWs which is crucial for understanding and optimizing the structural and optical properties of devices based on nitride NWs.

II. EXPERIMENT

A. Growth

GaN nanowires with single $Al_xGa_{1-x}N$ segments and accompanying Al-rich shell surrounding the lower part of the NW are grown on *in-situ* nitradated Si (111) substrates by PAMBE method in a Riber Compact 21 system with an elemental source of Ga and Al and an Addon RF plasma source of active nitrogen. No catalyst is used to induce nucleation of the NWs. The investigated nanowires with $Al_xGa_{1-x}N$ segments are grown in the following procedure. The GaN nanowire (which we call the base) is grown on the Si substrate. Then, an $Al_xGa_{1-x}N$ nanowire is grown on the top of the GaN base. The base is simultaneously covered with an Al-enriched $Al_xGa_{1-x}N$ shell. This is followed by the growth of a GaN nanowire (we call it the top) again. Composition of the $Al_xGa_{1-x}N$ inset has been changed in subsequent samples by changing the Al to Ga fluxes ratio (the N flux was kept constant) to obtain $x = 0.2$, 0.5, and 1. The average Al content in the insets, as measured by TEM-EDX technique for a number of NWs from each sample, corresponds well to the expected values and is equal to 0.22 ± 0.05, 0.49 ± 0.05, and 1, respectively. A sample with the nanowires formed of GaN only has been grown as a reference. Each of the studied samples was grown under highly N-rich conditions with the N/III ratio ~7, at temperature of 760 °C (determined in separate experiments as the optimum temperature for GaN/$Al_xGa_{1-x}N$ nanowire growth). To avoid intermixing on the GaN-$Al_xGa_{1-x}N$ interfaces, between each segment of the nanowire, a growth interruption and exposure to the nitrogen flux are applied. More details on the growth method used for fabrication of the NW structures can be found in Refs. 15 and 16.

B. Measurement techniques

Morphology, structure, and luminescence properties of the NWs are examined with the use of a field-emission SEM Hitachi SU-70 equipped with a Gatan MonoCL 3 cathodoluminescence system. The main body of experimental work is based on cathodoluminescence measurements. SEM combined with CL enables a direct correlation of luminescence maps and sample morphology at the nanoscale. High spatial and spectral resolution and high energy excitation make this method a perfect tool to study the optical properties of nanostructures which emit light in the UV range.[11,17] For studying local optical properties of each part of the nanowire, the NWs are removed from the original substrate and dispersed onto silicon wafers. Individual NWs are studied by CL spectroscopy and imaging at 80 K using an acceleration voltage of 5 kV and a beam current of 1.44 nA. CL "line scan" mode with a CCD camera is used to collect the luminescence spectra from the NW excited with the electron beam point by point along the specified line. The spatial resolution of the CL mapping is markedly improved for thin objects, such as nanowires. The electron beam defocusing occurring due to electron scattering along the relatively short path of the beam in the nanowire is substantially weaker than that for a quasi-infinite bulk sample (as shown in the inset of Fig. 1). Therefore, the CL signal comes mostly from the narrow region just around the path of the primary electron beam. Monte Carlo simulation of the CL intensity distribution, done with the use of the Casino v2.48 (2.4.8.1) software,[18] allows us to estimate the size of this region. Fig. 1 shows that about 60% of the CL signal from a nanowire with the thickness of 50 nm comes from the region with the diameter of 20 nm. This determines the resolution of CL imaging along the nanowire. The resolution across the NW is limited to the NW diameter.

TEM investigations of the NW structure and quantitative composition analysis are conducted with Titan 80–300

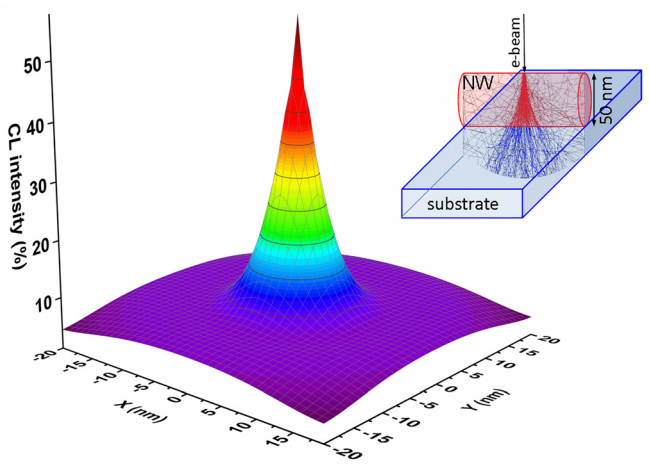

FIG. 1. The percentage of the emitted CL signal plotted as a function of the distance from the point excited with the electron beam in the GaN nanowire with the thickness of 50 nm (the result of the Monte Carlo simulation done with the use of the Casino v2.48 (2.4.8.1) software[18]). The inset shows schematically the paths of the primary electrons in the nanowire with diameter markedly shorter than the range of primary electron in the nanowire material.

Cubed high resolution transmission electron microscope operating at 300 keV, equipped with an EDAX Si(Li) energy dispersive X-ray (EDX) detector for X-ray microanalysis. HRXRD measurements allow the determination of the values of lattice parameters of the GaN/$Al_xGa_{1-x}N$ NW heterostructures. $2\theta/\omega$ scans are measured by a high-resolution "X'Pert PRO MRD XL" diffractometer with a standard four-bounce Ge(220) monochromator and three bounce (022) channel cut Ge analyzer crystal along with a 1.6 kW X-ray tube with CuKα1 radiation and vertical line focus.

III. RESULTS AND DISCUSSION

Imaging with the use of SEM and TEM shows that the typical NWs are ~600 to 800 nm long, with a diameter of ~30 to 50 nm. It is also confirmed that the length of the $Al_xGa_{1-x}N$ inset is equal to ~70 to 100 nm in each of the studied samples. In Fig. 2, cross-sectional (a) and plane-view (b) SEM images of a GaN/$Al_{0.49}Ga_{0.51}N$ nanowire sample are presented. For all samples (with various Al contents in the insets), the NWs grow along the c-axis normal to the Si(111) substrate surface and exhibit a very similar morphology.

The growth of a nanowire with $Al_xGa_{1-x}N$ segment leads to the formation of a shell around the GaN base of the NW. The $Al_xGa_{1-x}N$ shell surrounding the GaN-base of the NW may have higher Al content than the $Al_xGa_{1-x}N$ section due to the higher incorporation rate of Al at NW sidewalls, caused by much shorter diffusion length of Al adatoms, as compared to Ga ones.[6,12] Al atoms delivered to the side walls do not diffuse to the top facet and remain at the side walls, which leads to a lateral growth of the $Al_xGa_{1-x}N$ inset together with its axial growth. In samples with AlN sections, a pure AlN shell is formed around the GaN base. TEM images (Fig. 2(c)) show that the thickness of the shell increases from the bottom of the NW towards the top and reaches the maximum just below the inset with the values of 4.5 ± 2 nm, 8.2 ± 1.3 nm, and 12.0 ± 3.0 nm for NWs with $Al_{0.22}Ga_{0.78}N$, $Al_{0.49}Ga_{0.51}N$ and AlN insets, respectively. So, the corresponding values for the shell thickness are below the limit for plastic relaxation.[9] The AlN shell thickness is smaller than the length of AlN segment (70–100 nm) by 6–7 times. This difference becomes even higher for $Al_xGa_{1-x}N$ with lower x. This is due to the marked difference in the growth rate along and perpendicular to the [111] direction.

No intermixing between $Al_xGa_{1-x}N$ and GaN at the interface, as mentioned in the literature,[6,19] is observed in TEM-EDX measurements. The composition fluctuations similar to those reported in Ref. 20 have also not been revealed.

To study local optical properties, CL spectrum line scans have been recorded for a number of individual NWs from each sample (the orientation of the line scans is illustrated in the insertion of Fig. 3). Representative results of this procedure are shown in Fig. 3. Set of spectra in the left panel corresponds to the CL line scan of a pure GaN NW (without $Al_xGa_{1-x}N$ section). The curves are dominated by emission centered at 3.46 eV (at T = 80 K), which can be ascribed to the radiative recombination of excitons, present along the whole length of the NW. At temperature of 80 K

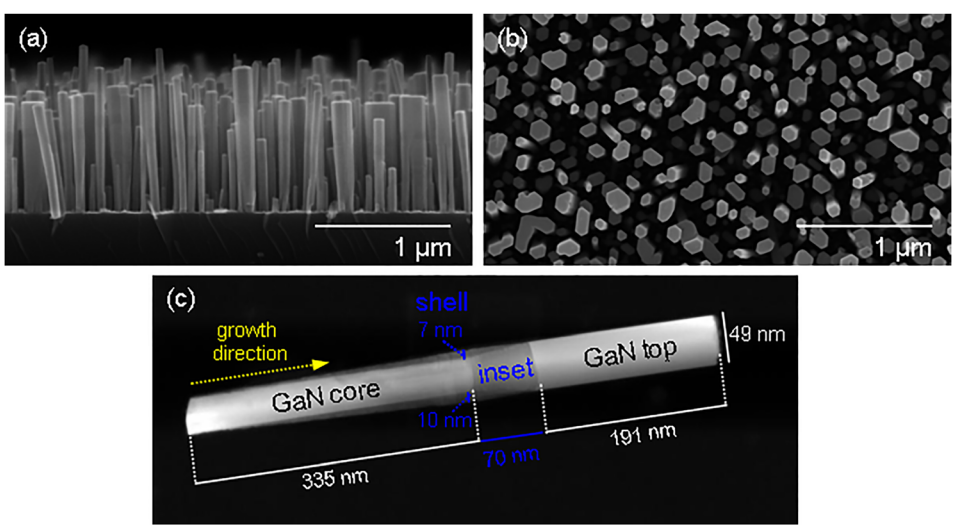

FIG. 2. Cross-sectional (a) and plane-view (b) SEM images and HAADF scanning TEM image (c) of the GaN/$Al_{0.49}Ga_{0.51}N$ NWs. In the TEM image, the dimensions of the NW parts are indicated.

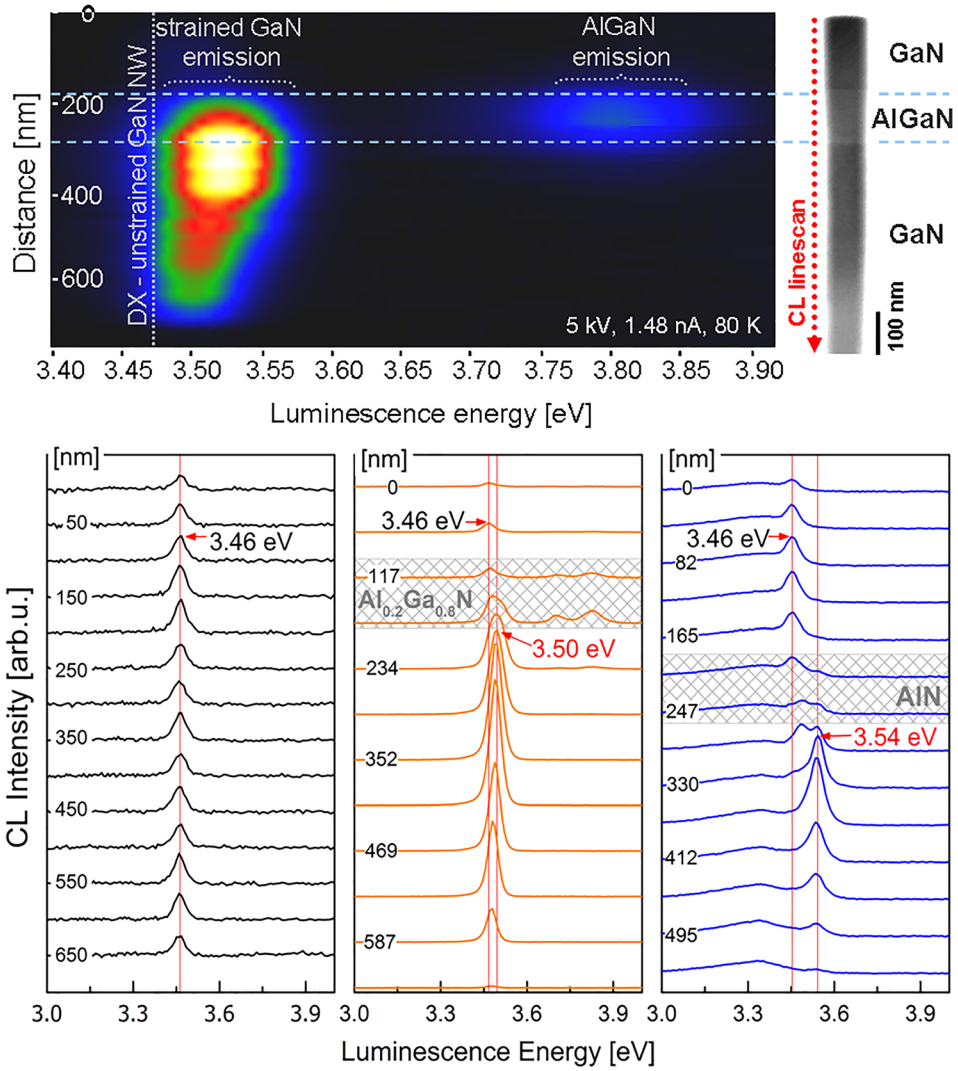

FIG. 3. Top panel: CL spectrum image (line scan) taken along individual GaN/$Al_{0.2}Ga_{0.8}N$ NW with discernible continuous change in compressively strained GaN core emission; the emission from the top part of NW is too weak to be reproduced in this intensity scale; the orientation of the CL line scan with respect to NW (from the top to the base of the NW) is indicated at the STEM image of NW. Bottom panel: Sets of spectra acquired for line scans of individual (from the left) GaN NW, and NWs with $Al_{0.22}Ga_{0.78}N$ and AlN insets and shells.

and relatively high excitation density in the CL experiment, one has to take into account the contributions from recombination of free A excitons as well as of donor bound ones[21] which, however, cannot be resolved in the recorded spectra.

The middle and right panels show the spectra of NW heterostructures with $Al_{0.2}Ga_{0.8}N$ and AlN sections, respectively. Both of them are dominated by a strong near-band-edge (NBE) luminescence of GaN within the core-shell region, which is blue-shifted in comparison with the luminescence of a pure GaN NWs. The blue-shift of luminescence energy increases from the bottom of the NW and reaches the maximum just below the $Al_xGa_{1-x}N$ inset. Such a progressive blue-shift of luminescence from the core-shell system can be interpreted as a consequence of an increasing compressive strain induced in the core by the shell with increasing thickness.[10] In the inset region, NBE luminescence of $Al_{0.22}Ga_{0.78}N$ and $Al_{0.49}Ga_{0.51}N$ was observed at energies of 3.83 eV and 4.44 eV, respectively. In the area of the GaN-top (above the $Al_xGa_{1-x}N$ sections), a luminescence of unstrained GaN is observed. It is markedly weaker than the emission of the GaN-core below the $Al_xGa_{1-x}N$ sections where nonradiative recombination centers related to the surface states are passivated by the Al-rich shell.[22] A strong, surface related nonradiative recombination can also be the reason why the luminescence of $Al_xGa_{1-x}N$ shell is not observed in our experiments.

The results of the CL studies are summarized in Fig. 4. The luminescence peak energies of GaN-cores and $Al_xGa_{1-x}N$ insets are displayed as a function of the Al content in the $Al_xGa_{1-x}N$ inset. The photon energy of luminescence from $Al_xGa_{1-x}N$ segments increases with the increase in the Al content, as expected for the solid solutions with the increasing fundamental energy gap. The increase rate is similar to that observed in the photoluminescence studies of relaxed epitaxial films at T = 4 K by Meyer *et al.*,[23] although the mean energy values determined for NWs in our experiments are systematically lower by 0.15–0.2 eV. The temperature difference between 4 and 80 K does not account for the energy difference of that magnitude.[23] We can only ascribe it to a discrepancy of $Al_xGa_{1-x}N$ composition determination or the presence of residual tensile strain existing in the $Al_xGa_{1-x}N$ segments of NWs, although the segments with the thickness of about 100 nm should be mostly relaxed.[9]

The blue-shift of the GaN-core luminescence increases with the Al content in the $Al_xGa_{1-x}N$ inset. A slight variation in the GaN-core emission for different NWs on one

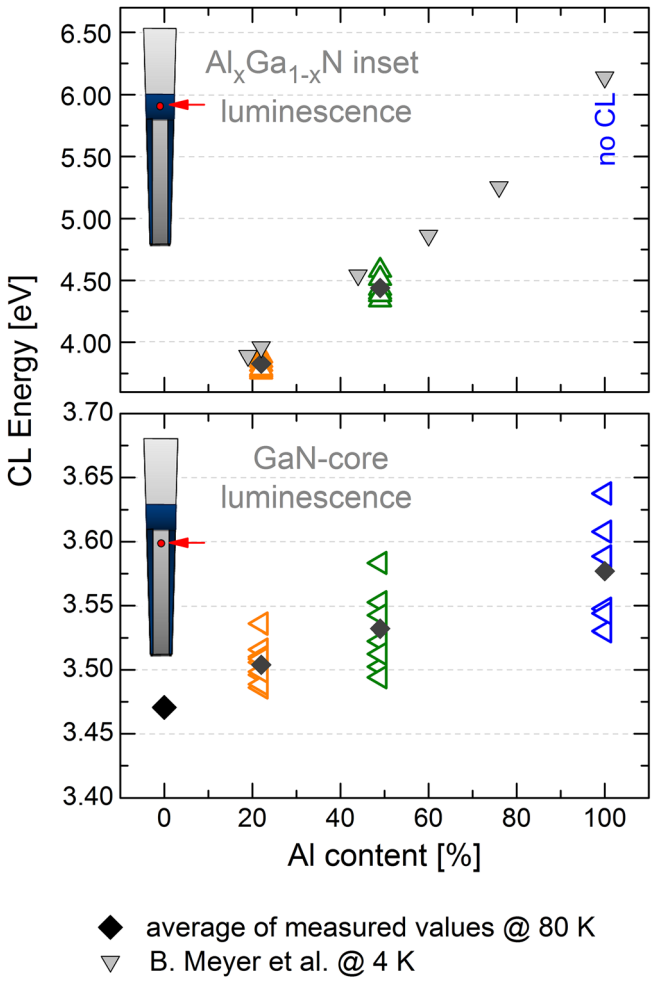

FIG. 4. Dependence of GaN-base/core and $Al_xGa_{1-x}N$ inset luminescence energies as a function of the Al content in the inset. The open triangles show the energies measured for individual NWs, the full diamonds—average values calculated for all investigated NWs. Insertions indicate the parts of NW that are excited by the electron beam in the CL experiments.

sample, increasing with the Al content, can be related to inhomogeneities of the core/shell thickness ratio and the composition of the shell. A chemical inhomogeneity in $Al_xGa_{1-x}N$ can be associated with influence of strain on the Al-Ga exchange mechanism[19] as well as kinetic effects during the growth.[6]

It has been proved for GaN/AlN core-shell nanowires[10] that the strain state in such a heterostructure is mainly determined by the component ε_{zz} along the nanowire c-axis. This quantity is negative in the compressively strained GaN-core and positive in the tensile-strained AlN shell. Since the contribution of the in-plane component is much lower, $\varepsilon_{xx} + \varepsilon_{yy} \ll \varepsilon_{zz}$, we can reasonably assume that the strain is purely uniaxial.[10]

For GaN, it was predicted theoretically[24] and confirmed by the results of experiments[10,25,26] that the increase in the compressive strain $|\varepsilon_{zz}|$ led to a blue-shift of the excitonic emission lines. The shift is proportional to ε_{zz} via the deformation potentials. So, if we compare the average values of CL emission energies and HRXRD results, a relationship between the blue-shift of the CL luminescence and a compressive out-of-plane strain in the GaN-core can be found.

To determine the strain state in the GaN-core, $2\theta/\omega$ scans of the 0002 reflection for the NW ensembles are measured. The c-lattice parameters of the GaN-top layer, GaN-core, $Al_xGa_{1-x}N$ inset, and $Al_xGa_{1-x}N$ shell are derived from the experimental data. The contributions from the GaN-top, GaN-core, $Al_xGa_{1-x}N$ inset, and the $Al_xGa_{1-x}N$ shell are revealed by fitting the $2\theta/\omega$ diffraction curve with Gaussian functions, as shown in Fig. 5 for GaN NWs with the AlN inset. Next, the values for the strain along the [0001] direction (ε_{zz}) in GaN-core are calculated using the following formula:[16]

$$\varepsilon_{ZZ} = \frac{c_{GaN-core} - c_{relax}}{c_{relax}},$$

where $c_{GaN\text{-}core}$ is the experimentally determined lattice parameter of the GaN-core and c_{relax} is the lattice parameter of relaxed GaN. Then, we calculate the stress using Hooke's law for a uniaxial strain with the value of Young's modulus for GaN nanowires equal to 227 GPa.[27]

Finally, a comparison of the mean values of CL energies measured for the sets of individual NWs with the results of HRXRD studies gives a relationship between the blue-shifted CL energy and a compressive out-of-plane strain (or corresponding stress) in the GaN core of investigated NWs (Fig. 6).

The obtained CL energy vs. strain dependence corresponds satisfactorily well to the results of high pressure photoluminescence experiments on wurzite GaN reported by Steube *et al.*[28] (Fig. 6 (top panel)), although we have to take into account that those results were obtained under hydrostatic pressure. Our results can also be compared well with the calculated results of Rigutti *et al.*[10] on the dependence of the GaN exciton energies on ε_{zz} strain. For x = 0.22 and 0.49, the mean energy values calculated for the whole sets of investigated NWs deviate from the curve describing the shift

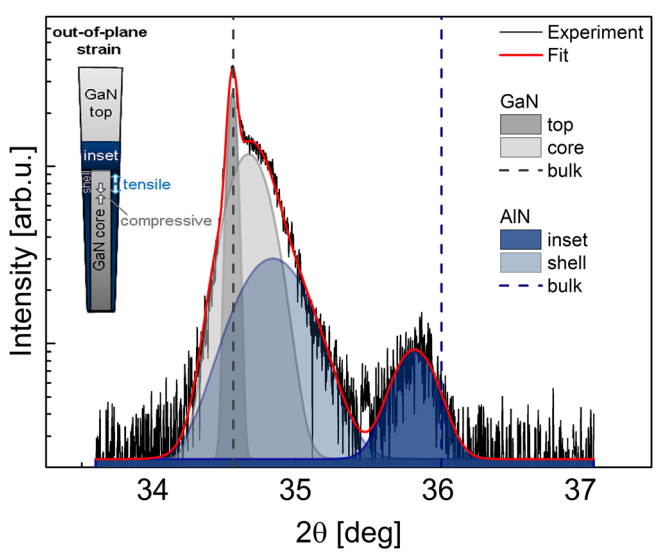

FIG. 5. The HRXRD $2\theta/\omega$ scan of 0002 reflection for an ensemble of GaN/AlN NWs with the result of a deconvolution into Gaussian singlets ascribed to diffraction from the parts of NW. Insertion shows the NW scheme with marked GaN-top, GaN-core, AlN inset, AlN shell, and strains assumed for the XRD spectra analysis.

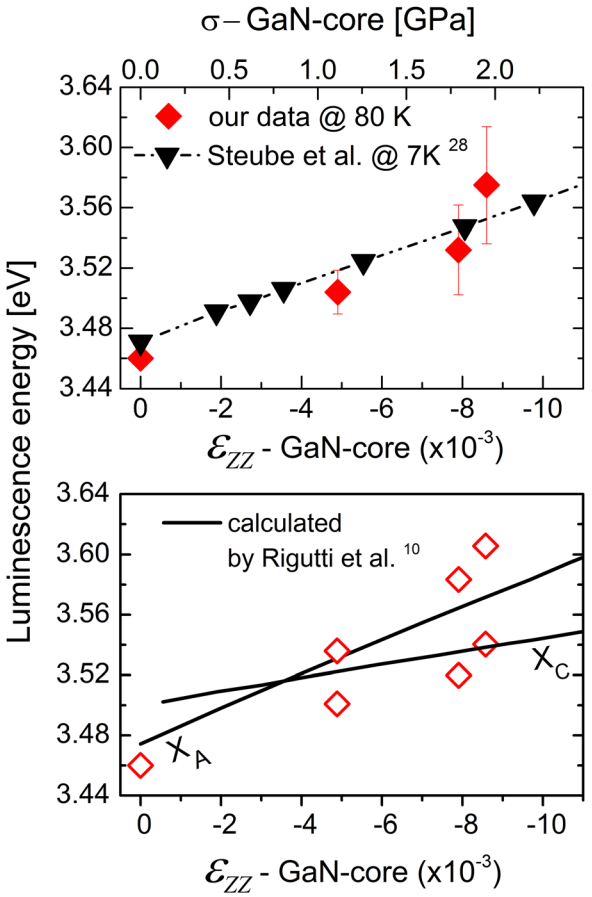

FIG. 6. CL energy vs. out-of-plane strain (or stress) in GaN core of NWs (mean values for the whole set of NWs (full symbols) or for two subsets of NWs (open symbols)) compared with the high pressure photoluminescence data[28] (top panel) and calculated shifts of the GaN A and C exciton lines[10] (bottom panel).

of A exciton line. They can perhaps be ascribed to the decay of C excitons, as observed for GaN/AlN nanowires and $\varepsilon_{zz} < -0.005$.[10] For the NWs with AlN sections, the observed CL peak energies cluster into two distinct groups (see Fig. 3) with the mean values of 3.54 and 3.60 eV. If we also plot separately the positions of the CL peaks observed at explicitly higher energies for a few NWs of $x = 0.22$ or 0.49 (open symbols in Fig. 6 (bottom panel)), we reveal that for $\varepsilon_{zz} < -0.005$ most of the experimental points follow the line expected for the C exciton, as in Ref. 10, while a minority still follow the line for the A exciton. The explanation of this observation needs further structural studies of those NWs which exhibit the peculiar optical properties. We can expect that structural deviations will lead to more complex strain distribution than described by the simplified model that has been considered in this study.

IV. SUMMARY AND CONCLUSIONS

The set of samples with GaN nanowires containing single $Al_xGa_{1-x}N$ segments with Al contents covering the whole composition range ($x = 0.0$, 0.22, 0.49, 1.0) are grown on *in-situ* nitradated Si(111) substrates by a catalyst-free PAMBE method. During the growth of $Al_xGa_{1-x}N$ segments, a shell around the GaN-base of NW is formed with relatively higher Al content. Its thickness and composition depend on the composition of the $Al_xGa_{1-x}N$ segment. Cathodoluminescence studies have shown a strong blue-shifted NBE emission of GaN in the core-shell region. Its average energy changes from 3.46 eV for GaN NWs to 3.50–3.57 eV in the core-shell structures depending on the Al content in the $Al_xGa_{1-x}N$ segment and in the shell. The acquired results prove that the blue-shift of the CL energy is a monotonic function of the $Al_xGa_{1-x}N$ composition. XRD studies revealed the presence of an out-of-plane (parallel to the c axis of NWs) compressive strain in the GaN-core. It corresponds to the stress from 1.1 GPa (for samples with $Al_{0.22}Ga_{0.78}N$ inset) to almost 2 GPa (for AlN). The comparison of the average values between the CL energies and XRD results allowed us to find a relationship between the blue-shift of the CL and a compressive out-of-plane strain in the GaN-core. For most of NWs, it follows the evolution expected for the GaN core under a uniaxial compressive strain along the axis of the structure; that is, for $\varepsilon_{zz} > -0.005$, the CL peak photon energy increases as expected for the GaN A exciton, for $\varepsilon_{zz} < -0.005$—for the C exciton, as in Ref. 10 for NWs with purely AlN insets.

Our investigations of GaN/$Al_xGa_{1-x}N$ NWs proved that the luminescence energy of the GaN core overgrown by the $Al_xGa_{1-x}N$ shell can be described as a smooth, monotonic function of the Al content in the whole range of x, at least if the thickness of the shell does not exceed 12 nm. For the shell made of the solid solution, there are two related factors governing the stress imposed on the core: the solid solution composition and the shell thickness. Fortunately, these factors acting simultaneously lead to a regular change of a strain in the core and the energy of optical emission from it. Our results show that such dependence can be relatively easily determined. Then, it can be used in the design of, for example, micro-LEDs in NWs, where the composition of $Al_xGa_{1-x}N$ layers is an important independent variable governing basic parameters of the whole device.

ACKNOWLEDGMENTS

The authors wish to thank Mr. H. Stanchu (V. Lashkaryov Institute of Semiconductor Physics, Kyiv, Ukraine) and Dr. J. Domagala (IP PAS, Warsaw, Poland) for the help with XRD measurements. This work was partly supported by the Polish National Science Centre (NCN) Grant No. DEC-2012/07/B/ST5/02484 and European Regional Development Fund No. POIG.02.01-00-14-032/08.

[1]M. A. Reshchikov and H. Morkoç, J. Appl. Phys. **97**, 061301 (2005).
[2]N. Thillosen, K. Sebald, H. Hardtdegen, R. Meijers, R. Calarco, S. Montanari, N. Kaluza, J. Gutowski, and H. Lüth, Nano Lett. **6**(4), 704 (2006).
[3]O. Brandt, C. Pfüller, C. Chèze, L. Geelhaar, and H. Riechert, Phys. Rev. B **81**, 045302 (2010).
[4]D. Zubia and S. D. Hersee, J. Appl. Phys. **85**(9), 6492 (1999).
[5]J. Ristić, E. Calleja, A. Trampert, S. Fernández-Garrido, C. Rivera, U. Jahn, and K. H. Ploog, Phys. Rev. Lett. **94**, 146102 (2005).
[6]C. Himwas, M. den Hertog, L. S. Dang, E. Monroy, and R. Songmuang, Appl. Phys. Lett. **105**, 241908 (2014).

[7]L. F. Zagonel, L. Rigutti, M. Tchernycheva, G. Jacopin, R. Songmuang, and M. Kociak, Nanotechnology **23**, 455205 (2012).
[8]S. Raychaudhuri and E. T. Yu, J. Appl. Phys. **99**, 114308 (2006).
[9]K. Hestroffer, R. Mata, D. Camacho, C. Leclere, G. Tourbot, Y. M. Niquet, A. Cros, C. Bougerol, H. Renevier, and B. Daudin, Nanotechnology **21**, 415702 (2010).
[10]L. Rigutti, G. Jacopin, L. Largeau, E. Galopin, A. De Luna Bugallo, F. H. Julien, J.-C. Harmand, F. Glas, and M. Tchernycheva, Phys. Rev. B **83**, 155320 (2011).
[11]A. Gustaffson, J. Microsc. **262**, 134 (2016).
[12]A. Pierret, C. Bougerol, M. den Hertog, B. Gayral, M. Kociak, H. Renevier, and B. Daudin, Phys. Status Solidi RRL **7**(10), 868 (2013).
[13]A. Pierret, C. Bougerol, B. Gayral, M. Kociak, and B. Daudin, Nanotechnology **24**, 305703 (2013).
[14]A. Pierret, C. Bougerol, S. Murcia-Mascaros, A. Cros, H. Renevier, B. Gayral, and B. Daudin, Nanotechnology **24**, 115704 (2013).
[15]M. Sobanska, K. P. Korona, Z. R. Zytkiewicz, K. Klosek, and G. Tchutchulashvili, J. Appl. Phys. **118**, 184303 (2015).
[16]A. Wierzbicka, Z. R. Zytkiewicz, S. Kret, J. Borysiuk, P. Dluzewski, M. Sobanska, K. Klosek, A. Reszka, G. Tchutchulashvili, A. Cabaj, and E. Lusakowska, Nanotechnology **24**, 035703 (2013).
[17]G. Yacobi and D. B. Holt, J. Appl. Phys. **59**(4), R1 (1986).
[18]D. Drouin, A. R. Couture, D. Joly, X. Tastet, V. Aimez, and R. Gauvin, Scanning **29**, 92 (2007).
[19]A. V. Kuchuk, V. P. Kladko, T. L. Petrenko, V. P. Bryksa, A. E. Belyaev, Yu. I. Mazur, M. E. Ware, E. A. DeCuir, Jr., and G. J. Salamo, Nanotechnology **25**, 245602 (2014).
[20]M. Belloeil, B. Gayral, and B. Daudin, Nano Lett. **16**, 960 (2016).
[21]C. Hauswald, P. Corfdir, J. K. Zettler, V. M. Kaganer, K. K. Sabelfeld, S. Fernandez-Garrido, T. Flissikowski, V. Consonni, T. Gotschke, H. T. Grahn, L. Geelhaar, and O. Brandt, Phys. Rev. B **90**, 165304 (2014).
[22]N. Sköld, L. S. Karlsson, M. W. Larsson, M-E. Pistol, W. Seifert, J. Trägårdh, and L. Samuelson, Nano Lett. **5**(10), 1943 (2005).
[23]B. K. Meyer, G. Steude, A. Göldner, A. Hoffmann, H. Amano, and I. Akasaki, Phys. Status Solidi B **216**(1), 187 (1999).
[24]S. L. Chuang and C. S. Chang, Phys. Rev. B **54**, 2491 (1996).
[25]S. Ghosh, P. Waltereit, O. Brandt, H. T. Grahn, and K. H. Ploog, Phys. Rev. B **65**, 075202 (2002).
[26]R. Ishii, A. Kaneta, M. Funato, Y. Kawakami, and A. A. Yamaguchi, Phys. Rev. B **81**, 155202 (2010).
[27]C.-Y. Nam, P. Jaroenapibal, D. Tham, D. E. Luzzi, S. Evoy, and J. E. Fischer, Nano Lett. **6**(2), 153 (2006).
[28]M. Steube, K. Reimann, O. Brandt, H. Yang, and K. H. Plogg, Phys. Status Solidi B **211**(1), 57 (1999).